Electronic Supplementary Material (ESI) for Chemical Communications.

Supporting Information

Robust Formation of Discrete Non-Covalent Pyrene Dimers in Amorphous Film by Strong π-π Interaction

Xiangyu Zhang,[a] Zhiyuan Fu,[b] Xinyan Jiang,[c] Zhiqiang Yang,[a] Shiyin Wang,[a] Kai Wang,[b] Zhijun Wu,[c] Shi-Tong Zhang,[a] Haichao Liu*[a] and Bing Yang*[a]

SUPPORTING INFORMATION

Table of Contents

Experimental Procedures

Synthesis of 2,2'-(2-(pyren-1-yl)ethene-1,1-diyl)bis(benzo[d]thiazole) (Py=2BZT):

Pyrene-1-carbaldehyde (921 mg, 4 mmol), bis(benzo[*d*]thiazol-2-yl)methane (1355 mg, 4.8 mmol), and piperidine (2.7 mL, 30 mmol) were added in 40 ml ethanol. The mixture was allowed to react at room temperature for 8 h. After removing the solvent, the residue was dissolved in dichloromethane and concentrated in a vacuum. It was purified by silica gel chromatography (eluent solvents: petroleum ether and dichloromethane) and then by sublimation to afford the orange powder in 85% yield (1680 mg). ^{1}H NMR (500 MHz, DMSO-d_6, 25 ˚C, TMS): δ = 9.20 (s, 1H), 8.49 (d, J = 9.2 Hz, 1H), 8.40 (m, 2H), 8.35 (d, J = 9.3 Hz, 1H), 8.28 (d, J = 8.9 Hz, 1H), 8.21 (d, J = 7.9 Hz, 1H), 8.18 – 8.09 (m, 5H), 7.94 (d, J = 8.0 Hz, 1H), 7.89 (d, J = 8.0 Hz, 1H), 7.62 (t, J = 7.8 Hz, 1H), 7.55 (m, 2H), 7.44 (t, J = 7.6 Hz, 1H). ^{13}C NMR (126 MHz, $CDCl_3$, 25 ˚C, TMS): δ = 166.69 (C), 164.33 (C), 153.19 (C), 152.77 (C), 138.05 (CH), 136.15 (C), 132.13 (C), 131.27 (C), 130.97 (C), 130.37 (C), 130.21 (C), 129.25 (C), 128.58 (CH), 128.46 (CH), 127.89 (CH), 127.37 (CH), 126.46 (CH), 126.29 (CH), 126.20 (CH), 125.91 (CH), 125.82 (CH), 125.37 (CH), 124.82 (C), 124.73 (CH), 124.64 (C), 123.92 (CH), 123.78 (CH), 123.33 (CH), 121.56 (CH). FTIR (KBr, cm^{-1}): ν =: 3035, 1585, 1429, 1313, 1197, 1037, 923, 844, 760, 727 cm^{-1}; GC/MS, EI (mass m/z): 493.08; Elemental analysis calculated [%] for $C_{32}H_{18}N_2S_2$: C 77.70, H 3.67, N 5.66, S 12.96; found: C 77.56, H 3.90, N 5.51, S 13.03.

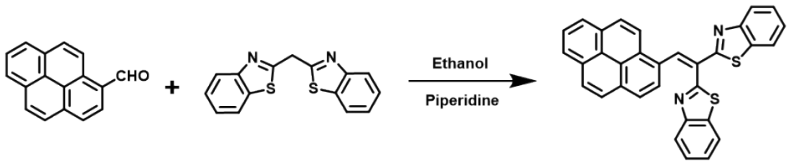

Scheme S1. Synthetic route of Py=2BZT molecule.

General Information

All the reagents and solvents used for the synthesis were purchased from Aldrich and Acros companies and used without further purification. The NMR data were recorded on a Bruker AVANCE 500 spectrometer at 500 MHz, and the tests used tetramethylsilane (TMS) as internal standard. DMSO-d_6 and $CDCl_3$ were selected as solvents for ^{1}H NMR and ^{13}C NMR respectively. The mass spectra (MS) were recorded using an ITQ1100 (Thermo Fisher). The compounds were characterized by a Flash EA 1112, CHNS elemental analysis instrument.

Spectroscopy measurements:

Fourier transform infrared (FT–IR) spectroscopy was carried out using a Bruker VERTEX 80V Fourier-transform infrared spectrometer. UV–vis spectra of solutions were recorded on a Shimadzu UV-3100 Spectrophotometer. Steady-state photoluminescence (PL) spectra, time-resolved PL spectra and temperature-dependent PL spectra were carried out by FLS980 Fluorescence Spectrometer by Edinburgh Instruments. PL spectra with various time delays were carried out by FLS1000 Fluorescence Spectrometer by Edinburgh Instruments.

Average lifetime was calculated using the following formula,[1] where A_i is the pre-exponential for lifetime τ_i.

$$\tau_{av} = \sum A_i \tau_i^2 / \sum A_i \tau_i$$

Thermal measurements:

Differential scanning calorimetry (DSC) analysis was carried out using a NETZSCH (DSC-204) instrument at a heating rate of 10 °C/min in nitrogen flow.

X-ray diffraction (XRD):

Single crystal X-ray diffraction experiments were carried out on a Rigaku R-AXIS RAPID diffractometer equipped with a Mo-Kα and control Software using the RAPID AUTO. The crystal structures were solved with direct methods and refined with a full-matrix least-squares technique using the Olex2 program. Powder XRD patterns were collected on a Rigaku SmartLab(3) diffractometer.

Theoretical calculation:

The highest occupied molecular orbital (HOMO) and the lowest unoccupied molecular orbital (LUMO) were obtained on the basis of density functional theory (DFT) method at the level of BMK/6-31G (d, p). Optimized excited state geometry and natural transition orbitals (NTOs) were calculated on the basis of time-dependent DFT (TD-DFT) method at the level of BMK/6-31G (d, p). All the DFT and TD-DFT calculations were carried out using Gaussian 09 (version D.01) package.[2] Transition density matrix (TDM) color-filled maps were obtained using Multiwfn software.[3]

High-pressure generation and optical measurements:

The high-pressure experiments were performed by the diamond anvil cell (DAC). The sample was placed in the T301 gasket hole with a diameter of 150 μm and a thickness of 40 μm. And a small ruby ball was placed next to the sample for in-situ pressure

calibration. In the high-pressure absorption and PL experiments, silicone oil (Aldrich) was used as the pressure-transition medium (PTM).

In-situ high-pressure PL and absorption photos of the samples were shot by Canon Eos 5D mark II equipped with Nikon Eclipse TI-U microscope. The absorption spectra light source adopted deuterium−halogen light source and the PL excitation source was the 355 nm line of a UV DPSS laser. The Spectrometer adopted Ocean Optics QE65000 spectrometer.

Results and Discussion

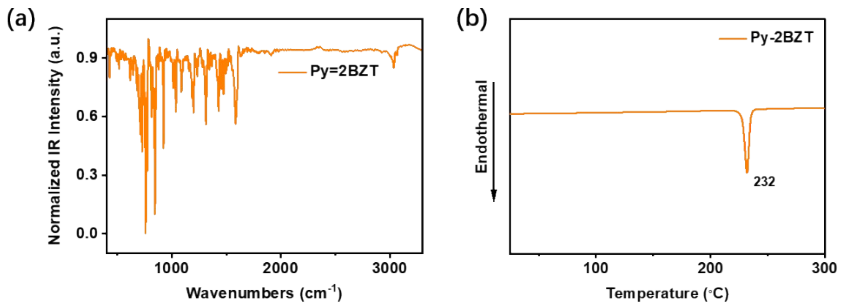

Figure S1. (a) IR spectrum and (b) DSC pattern of Py=2BZT crystal.

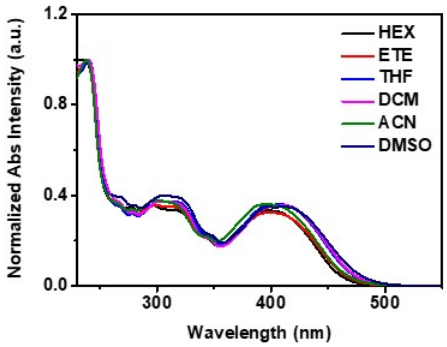

Figure S2. UV–vis absorption spectra of Py=2BZT in different solvents (HEX: hexane, ETE: ethyl ether, THF: tetrahydrofuran, DCM: dichloromethane, ACN: acetonitrile, DMSO: dimethyl sulfoxide).

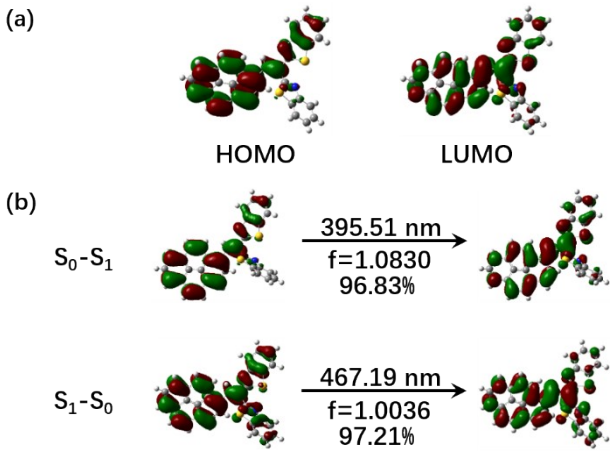

Figure S3. (a) HOMO and LUMO of Py=2BZT monomer based on ground state geometry directly obtained in crystal structure. (b) NTOs of S_0 and S_1 of Py=2BZT monomer based on ground state geometry directly obtained in crystal structure and optimized excited state geometry.

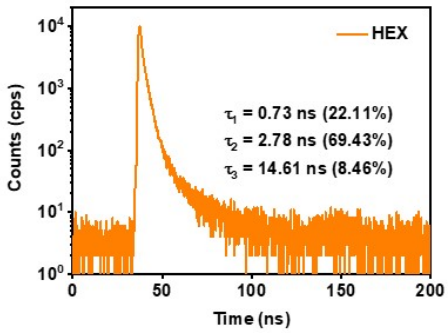

Figure S4. Time-resolved PL spectrum of Py=2BZT in diluted HEX solution (10^{-5} mol/L).

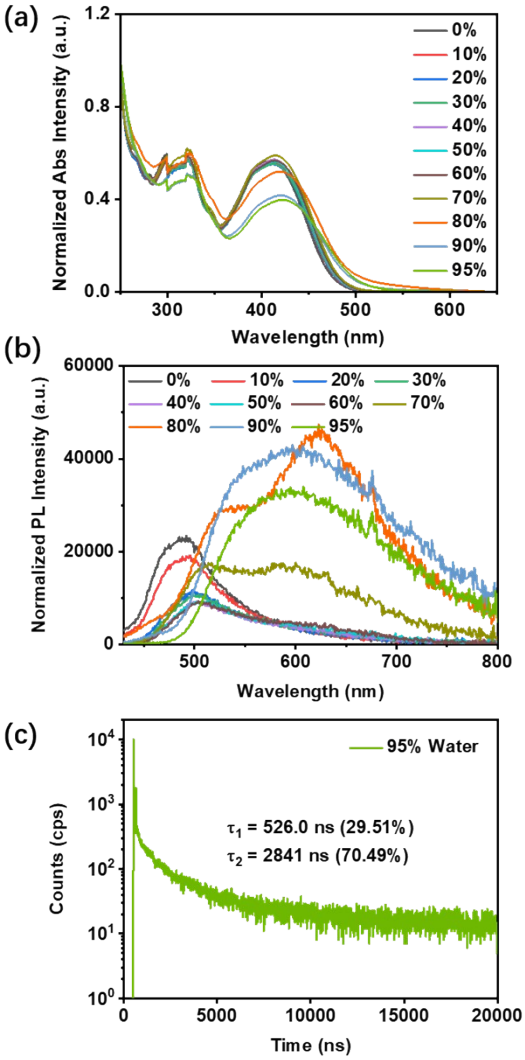

Figure S5. (a) UV-vis absorption spectra and (b) PL spectra of Py=2BZT in THF/water mixtures with different water contents. (c) Time-resolved PL spectra of Py=2BZT in THF/water mixture with water content of 95%.

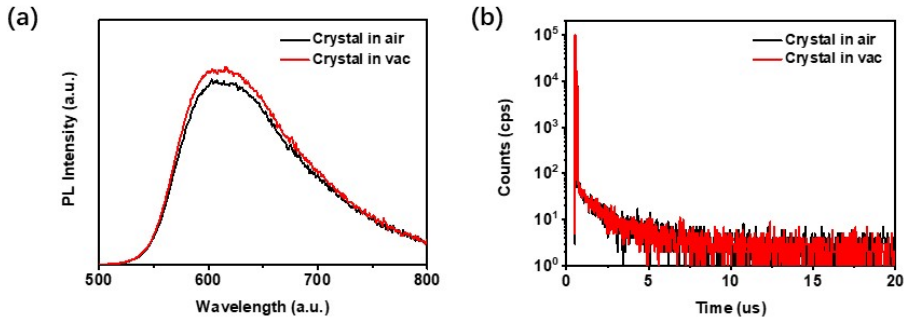

Figure S6. (a) PL spectra and (b) time-resolved PL spectra of Py=2BZT crystal in air and in a vacuum.

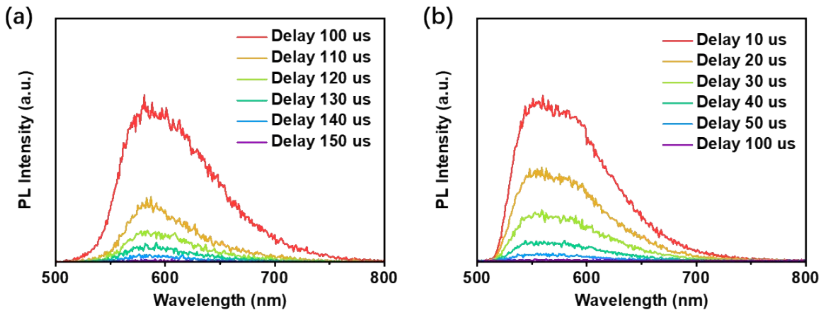

Figure S7. PL spectra of Py=2BZT crystal recorded at various time delays (a) at room temperature and (b) at 80 K.

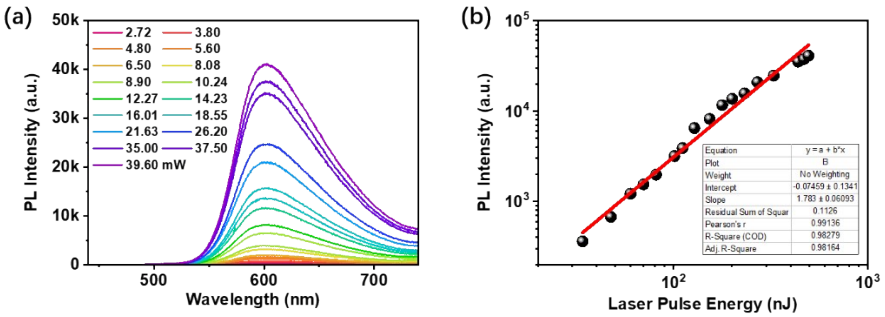

Figure S8. (a) PL spectra of Py=2BZT crystal under different excitation powers. (b) Double logarithmic plot of PL intensity measured as a function of laser pulse energy of Py=2BZT crystal.

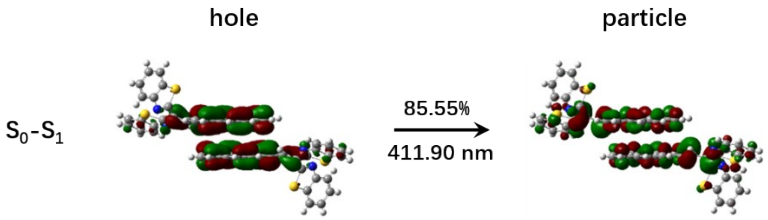

Figure S9: The NTOs for S_0 to S_1 of Py=2BZT dimer.

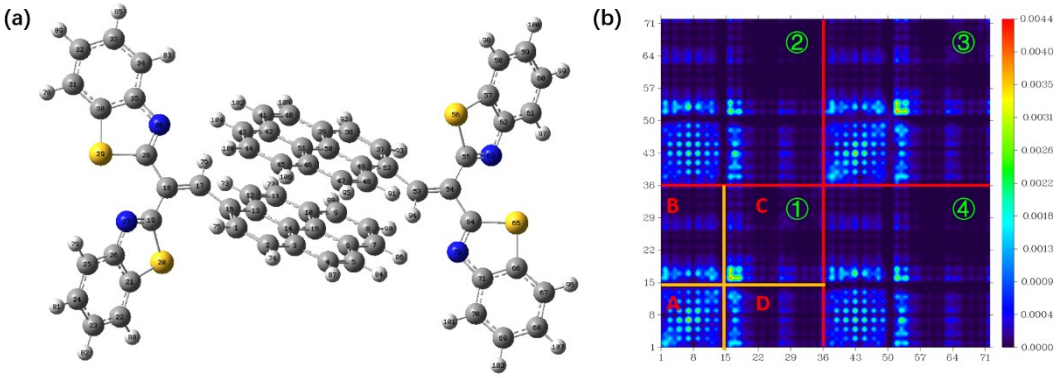

Figure S10. (a) Labels of atoms and (b) TDM color-filled map of the S_1 state of Py=2BZT dimer directly obtained from crystal structure.

Explanation of TDM color-filled maps:

For the two-dimension (2D) color-filled map, both the horizontal axis x_i and the vertical axis y_i run over all of the non-hydrogen atoms of dimer, shown as Figures S10b. Each coordinate point (x_i, y_i) was related to the probability $|\Psi(x_i, y_i)|^2$ of finding the electron and hole in the π-atomic orbitals of two non-hydrogen atoms x_i and y_i, respectively. The brightness of each coordinate point (x_i, y_i) is directly proportional to the probability of $|\Psi(x_i, y_i)|^2$. The area of diagonal of 2D color-filled map represents that electronic transition has a dominant locally-excited (LE) character, while the area of off-diagonal represents a charge-transfer (CT) character. For Py=2BZT dimer, its whole 2D color-filled map was divided into four areas by the red lines, which numbered as ①, ②, ③ and ④. The brightness in ① and ③ areas represent LE electronic transition of Py=2BZT monomer, and the brightness in ② and ④ represent CT electronic transition from a Py=2BZT molecule to another. What is more, the ① area, which stands for one Py=2BZT molecule in dimer, was taken as an example for further analysis. The whole ① area was divided into four areas by the orange lines, named as A, B, C and D, respectively. The brightness in A area represent LE electronic transition of Py unit, and the brightness in C area represent LE electronic transition of C=C bond and BZT units. The brightness in B and D areas represent CT electronic transition from Py unit to C=C bond and BZT units.

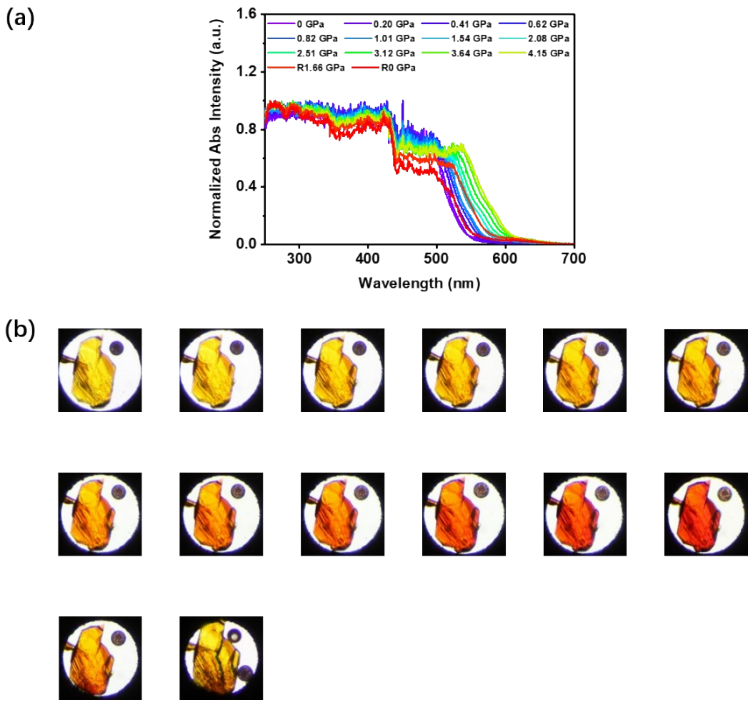

Figure S11. (a) UV–vis absorption spectra and (b) corresponding photographs of Py=2BZT crystal under different pressures.

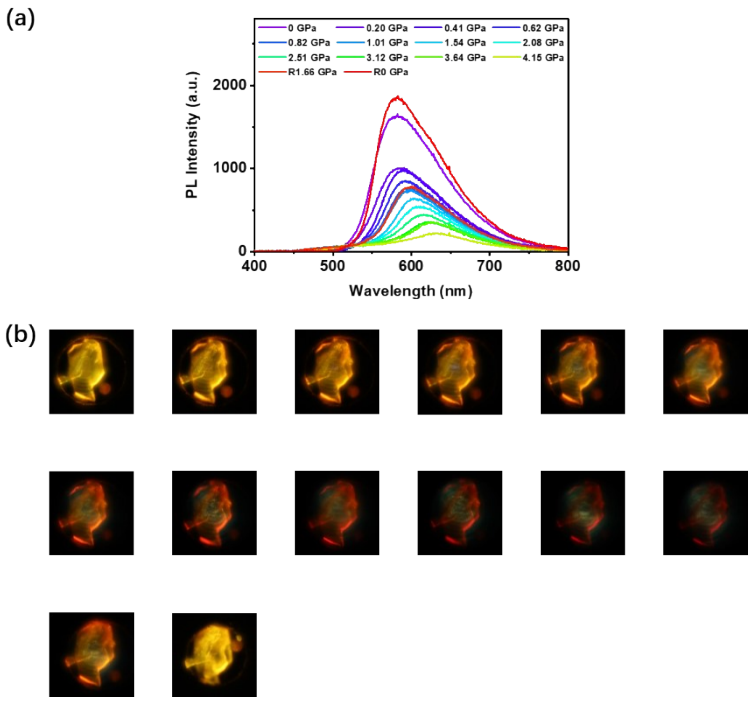

Figure S12. (a) PL spectra and (b) corresponding photographs of Py=2BZT crystal under different pressures.

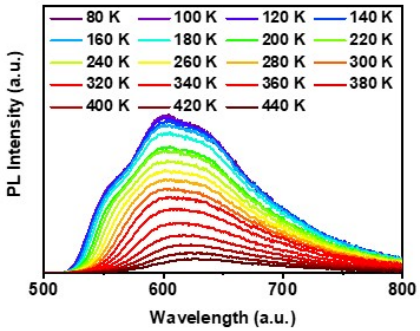

Figure S13. PL spectra of Py=2BZT crystal with increasing temperature from 80 K to 440 K in a vacuum (temperature gradient: 20 K)

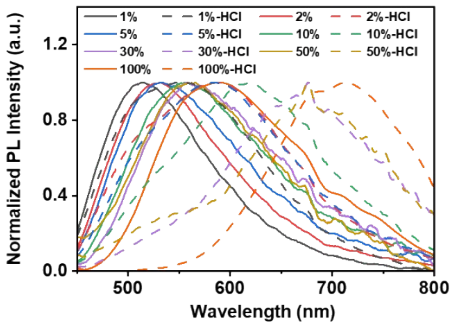

Figure S14. PL spectra of doped Py=2BZT films with different concentration in PMMA before (solid line) and after (dotted line) fumed by hydrochloric acid (HCl).

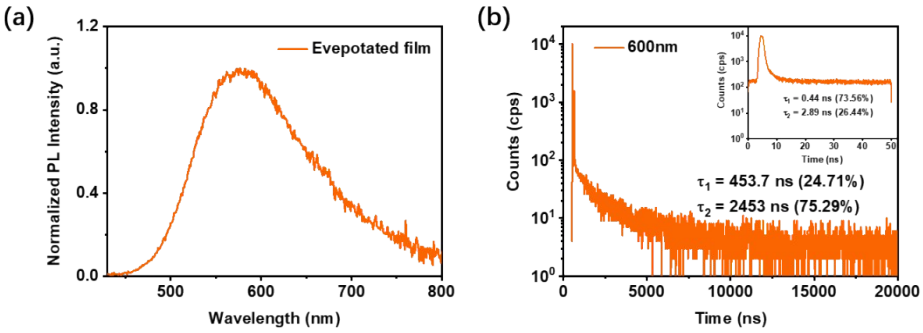

Figure S15. (a) PL and (b) time-resolved PL spectra of Py=2BZT film obtained by vacuum evaporation.

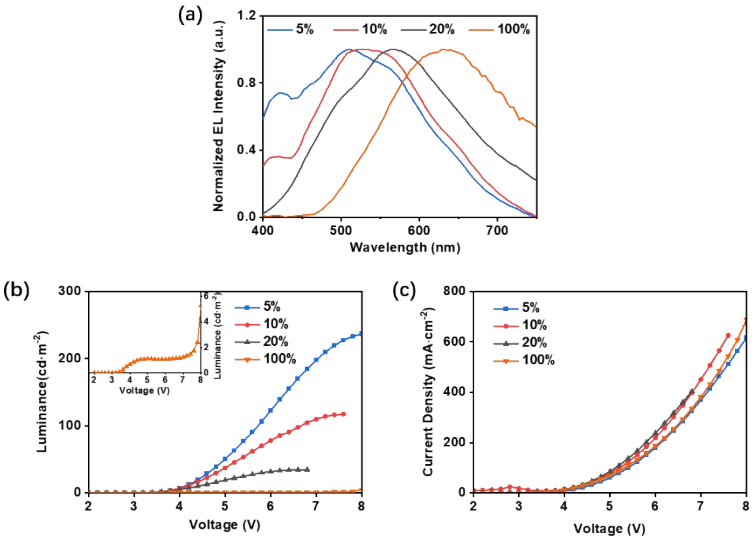

Figure S16. (a) EL spectra of Py=2BZT EL devices with different doped concentration in TCTA as host. The curves of (b) Luminance-Voltage and (c) Current Density-Voltage of Py=2BZT EL devices.

The devices were fabricated by vacuum evaporation and their structures are as follows:

5%: HAT-CN (5nm) / TAPC (25nm) / TCTA (10nm) / TCTA : Py=2BZT (5%,20nm) / TPBI(40nm) / LIF(1nm) / AL (120nm)

10%: HAT-CN (5nm) / TAPC (25nm) / TCTA (10nm) / TCTA : Py=2BZT (10%,20nm) / TPBI(40nm) / LIF(1nm) / AL (120nm)

20%: HAT-CN (5nm) / TAPC (25nm) / TCTA (10nm) / TCTA : Py=2BZT (20%,20nm) / TPBI(40nm) / LIF(1nm) / AL (120nm)

100%: HAT-CN (5nm) / TAPC (25nm) / TCTA (10nm) / Py=2BZT (20nm) / TPBI (40nm) / LiF (1nm) / AL (120nm)

Table S1. Crystallographic data of Py=2BZT.

	Py=2BZT
crystal color	orange
empirical formula	$C_{32}H_{18}N_2S_2$
formula weight	494.60
T [K]	293.0
crystal system	triclinic
space group	P -1
a [Å]	8.8249(7)
b [Å]	11.0232(9)
c [Å]	12.6120(11)
α [°]	68.065(3)
β [°]	81.235(3)
γ [°]	84.301(3)
V [Å^3]	1123.57(16)
Z	2
F(000)	512
density [g/cm^3]	1.462
μ [mm^{-1}]	0.264
reflections collected	4741
unique reflections	4311
R (int)	0.0253
GOF	1.028
R_1 [I>2σ(I)]	0.0291
$ωR_2$ [I>2σ(I)]	0.0758
R_1 (all data)	0.0332
$ωR_2$ (all data)	0.0798
CCDC number	2164118

References

[1] Q. Zhang, H. Kuwabara, W. J. Potscavage, Jr., S. Huang, Y. Hatae, T. Shibata, C. Adachi, *J. Am. Chem. Soc.* **2014**, 136, 18070-18081.

[2] M. J. Frisch, G. W. Trucks, H. B. Schlegel, G. E. Scuseria, M. A. Robb, J. R. Cheeseman, G. Scalmani, V. Barone, G. A. Petersson, H. Nakatsuji, X. Li, M. Caricato, A. V. Marenich, J. Bloino, B. G. Janesko, R. Gomperts, B. Mennucci, H. P. Hratchian, J. V. Ortiz, A. F. Izmaylov, J. L. Sonnenberg, D. Williams-Young, F. Ding, F. Lipparini, F. Egidi, J. Goings, B. Peng, A. Petrone, T. Henderson, D. Ranasinghe, V. G. Zakrzewski, J. Gao, N. Rega, G. Zheng, W. Liang, M. Hada, M. Ehara, K. Toyota, R. Fukuda, J. Hasegawa, M. Ishida, T. Nakajima, Y. Honda, O. Kitao, H. Nakai, T. Vreven, K. Throssell, J. A. Montgomery, Jr., J. E. Peralta, F. Ogliaro, M. J. Bearpark, J. J. Heyd, E. N. Brothers, K. N. Kudin, V. N. Staroverov, T. A. Keith, R. Kobayashi, J. Normand, K. Raghavachari, A. P. Rendell, J. C. Burant, S. S. Iyengar, J. Tomasi, M. Cossi, J. M. Millam, M. Klene, C. Adamo, R. Cammi, J. W. Ochterski, R. L. Martin, K. Morokuma, O. Farkas, J. B. Foresman, and D. J. Fox, Gaussian 09, Revision D.01, Gaussian, Inc., Wallingford CT, 2013.

[3] T. Lu and F. Chen, *J. Comput. Chem.* **2012**, 33, 580-592.